An Inverted Pendulum Model of Walking for Predicting Navigation Uncertainty of Pedestrian in Case of Foot-mounted Inertial Sensors

Chi-Shih Jao, Eudald Sangenis, Paula Simo, Alexandra Voloshina, Andrei M. Shkel
Department of Mechanical and Aerospace Engineering, University of California, Irvine
{chishihj,esangeni,psimohig,avoloshi,andrei.shkel}@uci.edu

***Abstract*—This paper presents a simplified model for predicting navigation uncertainty of a pedestrian. The model simulates trajectories of a person's foot, and these trajectories are then used to generate simulated IMU readings. Eight different noise errors are considered for both the simulated accelerometer and gyroscope readings, including white noise, bias instability, random walk, scale factor error, misalignment, turn-on bias, limited full-scale range, and limited bandwidth. We conducted a series of pedestrian walking experiments to validate the proposed model. The experimental results showed that the position Root-Mean-Square-Errors (RMSEs) in the simulations and in the experiments had a discrepancy of 6% for about 40 [m] of walk. The model also predicted the bounds of the vertical position drift, which matched the trend of estimated vertical position uncertainties in the experiments. We concluded that the model could predict, with sufficient accuracy, the navigation uncertainty for foot-mounted IMU-based systems, and we suggested future research to enhance the model with additional details of foot motion to further improve the prediction accuracy.**

***Index Terms*—IMU, ZUPT, walking simulation, navigation**

I. Introduction

Foot-mounted Inertial Navigation Systems (INS) have been considered as a promising technology for pedestrian navigation systems, which may enable a variety of critical Location-Based Services (LBS), including contact tracing, firefighter localization, and rehabilitation training. An INS uses self-contained measurements collected from Inertial Measurement Units (IMUs), operating seamlessly in environments where Global Navigation Satellite Systems (GNSS) are not available [1]. A foot-mounted configuration allows for enhancing the INS with a Zero velocity UPdaTe (ZUPT) algorithm that resets velocity errors during the stance phase of a gait cycle [2]. The ZUPT algorithm significantly reduces accumulated navigation errors of an INS and has been experimentally demonstrated to have a positioning error of less than 1% of traveling distances [3].

While evaluating the ZUPT-aided INS experimentally provides a realistic understanding of the system's navigation performance, it is challenging in experiments to isolate and investigate the contribution of error sources in the system. A simulation model for foot-mounted IMU-based navigation systems would be beneficial for characterization of sensor errors and could be used for prediction of the navigation accuracy, for example, using the Monte Carlo simulation incorporating sensors' uncertainty. Previous research developed such simulation models by first generating reference position trajectories of a pedestrian's foot, transforming the position information to simulated IMU readings, and considering different combinations of factors, including sensor white noises, bias instabilities, random walks, misalignment, scale factors, sampling rate, swing phase duration in a gait cycle, and stance phase detection performance, that have effects on navigation accuracy [4]–[7]. These models, however, are not suitable for considering errors caused by insufficient sensors' Full-Scale Range (FSR) and bandwidth, which are known to be significant contributors in foot-mounted navigation scenarios.

This work was performed under the following financial assistance awards: 70NANB22H073 from the U.S. Department of Commerce, National Institute of Standards and Technology (NIST).

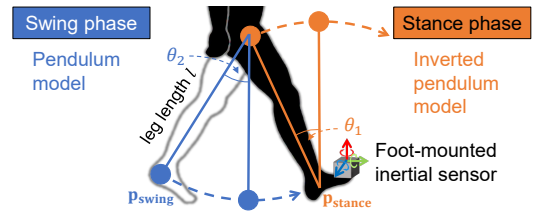

Fig. 1. Modeling of walking dynamics using an inverted pendulum in the stance phase and regular pendulum in the swing phase.

Traditional simulation models for foot-mounted INS simulated IMU measurements based on reference positions generated with motion capture cameras [5] or foot-mounted IMUs themselves [4], but it was found difficult to capture signals that have magnitudes larger than the sensors' FSR and frequencies higher than the sensors' sampling rate and bandwidth. One example of such signals is high accelerations due to mechanical shocks that occur during the heel-strike and toe-off phases, and these shocks could saturate FSRs and bandwidths of many consumer-grade IMUs [8]. The saturation needs to be modeled in a pedestrian navigation simulation to avoid predicting falsely optimistic navigation uncertainty of the ZUPT-aided INS [9]. A relatively simple dynamic analytical model that mimics swing and contact during the foot motions would be advantageous, allowing studying the effects of the high-frequency sampling of sensor readings and large-magnitude signals during foot swing and contact on navigation performance.

This paper presents an analytical model with reduced complexity based on an inverted pendulum shown in Fig. 1. This

model is used to generate foot position for the case of foot-mounted INS-based navigation. The proposed model accounts for high acceleration shocks during the heel-strike and toe-off phases, which enable simulating the effects of the limited sensor FSR and bandwidth on navigation accuracy. Additionally, six different IMU noise sources, including white noise, bias instability, random walk, scale factor inconsistencies, misalignment, and turn-on bias were added to the simulated IMU signals.

II. Approach

This section discusses our approach to modeling foot trajectories, foot-mounted IMU measurements, and IMU noise.

A. Rigid Body Walker

We used a walking model, referred to as the rigid body walker [10]–[12], and investigated whether such a model is capable of predicting with sufficient accuracy the trajectory of the foot during walking. Fig. 1 shows the configuration of the model, which consists of two rigid legs of length l of negligible mass connected by a frictionless hinge joint. The motion of the model is constrained to two dimensions. In this model, only one foot is on the ground at any given moment, during which time the system behaves like an inverted pendulum. The angle dynamics of the stance leg with respect to gravity, denoted as θ_1, are expressed as

$$\ddot{\theta_1} = \frac{g}{l}\sin(\theta_1),$$

where g is the gravity constant. The motion of the swing leg is dictated by the torsional hip spring, with a spring constant, k_{hip}, acting between the stance and swing legs. This is analogous to hip flexor and extensor muscle activity during healthy human walking. The angle of the swing leg, θ_2, with respect to gravity, is calculated as

$$\ddot{\theta_2} = \frac{k_{\text{hip}}}{m_f l^2}(\theta_1 - \theta_2) + \frac{g}{l}(\sin(\theta_1 - \theta_2)\cos(\theta_1)) - \dot{\theta_1}^2 \sin(\theta_1 - \theta_2),$$

where m_f is the mass of the foot. With $m_f \ll m$, the swing leg does not affect stance leg dynamics [13]. The model is simulated to be analogous to human walking at a speed of 1.00 [m/s] and a step length of 0.662 [m]. To obtain generalized results, all model parameters were non-dimensionalized with respect to body mass (m), leg length (l, $0.87\,\mathrm{m}$ for typical human) and gravity (g). As a result, the simulated model gait had an average speed, $\bar{v}$, of $\bar{v}$=0.342 $\sqrt{lg}$.

Initial conditions of the model are set such that model dynamics repeat with each step. In other words, the model is on a limit cycle and all system states are identical for each step. The roles of the swing and stance leg switch when the swing leg contacts the ground. At this point, the model undergoes a perfectly inelastic collision, which redirects the center of mass velocity to be tangential to the new stance leg. Energy is lost as a result of this collision and must be replaced in order to maintain steady-state walking. To compensate for the energy loss, an impulse is applied along the stance leg immediately prior to foot contact of the swing leg. In other words, the impulse is perpendicular to the CoM direction of motion before collision and is analogous to the push-off work done by the lower leg muscles during human walking [13].

The pelvis positions of the rigid body walker, $\mathbf{p}_{\text{pelvis}}$, during each step can be computed as

$$\mathbf{p}_{\text{pelvis}} = l \begin{bmatrix} -(\sin(\theta_1) - \sin(\theta_{1,0})) \\ 0 \\ \cos(\theta_1) \end{bmatrix} + \mathbf{p}_{\text{pelvis},0},$$

where $\mathbf{p}_{\text{pelvis},0}$ is the position of the pelvis at the end of the previous step and $\theta_{1,0}$ is the angle of the stance leg at the beginning of each step. Positions of the stance leg, $\mathbf{p}_{\text{stance}}$, and the swing leg, $\mathbf{p}_{\text{swing}}$, are computed as

$$\mathbf{p}_{\text{stance}} = \mathbf{p}_{\text{pelvis}} + l \begin{bmatrix} \sin(\theta_1) \\ 0 \\ -\cos(\theta_1) \end{bmatrix}, \mathbf{p}_{\text{swing}} = \mathbf{p}_{\text{pelvis}} + l \begin{bmatrix} \sin(\theta_2) \\ 0 \\ -\cos(\theta_2) \end{bmatrix}.$$

In our simulation, positions of a foot in the navigation frame, denoted as $\mathbf{p}^n$, are obtained by alternating between positions of the stance leg and the swing leg. Roll angle ϕ and yaw angle ψ of the foot remain zero throughout the entire simulation, and the pitch angle θ alternates between θ_1 and θ_2.

B. Synthesizing IMU Readings

This paper follows the strapdown INS algorithm, discussed for example in [1], and transforms the ground truth position $\mathbf{p}^n$ and orientations along roll ϕ, pitch θ, and yaw ψ angles generated from the rigid body walker to noise-free IMU signals. Velocities in the navigation frame $\mathbf{v}^n$ are computed from the position $\mathbf{p}^n$, and accelerations in the navigation frame $\mathbf{a}^n$are obtained from the velocity. Angular rates of the body frame with respect to the navigation frame $\boldsymbol{\omega}^b_{nb}$ are calculated from orientations as

$$\boldsymbol{\omega}^b_{nb} = \begin{bmatrix} \dot{\phi} \\ 0 \\ 0 \end{bmatrix} + \mathbf{C}_3 \begin{bmatrix} 0 \\ \dot{\theta} \\ 0 \end{bmatrix} + \mathbf{C}_3\mathbf{C}_2 \begin{bmatrix} 0 \\ 0 \\ \dot{\psi} \end{bmatrix},$$

where $\mathbf{C}_3$ is a rotation matrix rotating ϕ degree along the roll direction and $\mathbf{C}_2$ is a rotation matrix rotating θ degree along the pitch direction. Local gravity is computed as

$$\mathbf{g}^n_l = \mathbf{g} - \boldsymbol{\omega}^n_{ie} \times (\boldsymbol{\omega}^n_{ie} \times \mathbf{p}^n),$$

where $\mathbf{g}$ is the gravity vector and $\boldsymbol{\omega}^n_{ie}$ is the Earth rate. Noise-free accelerometer readings $\mathbf{u}_a$ are obtained as

$$\mathbf{u}_a = \mathbf{C}^b_n(\mathbf{a}^n + (2\boldsymbol{\omega}^n_{ie} + \boldsymbol{\omega}^n_{en}) \times \mathbf{v}^n + \mathbf{g}^n_l), \tag{1}$$

where $\boldsymbol{\omega}^n_{en}$ is the transport rate of the navigation frame and $\mathbf{C}^b_n$ is the Direction Cosine Matrix (DCM) representation of $\boldsymbol{\omega}^b_{nb}$. Noise-free gyroscope readings $\mathbf{u}_g$ are expressed as

$$\mathbf{u}_g = \boldsymbol{\omega}^b_{nb} + \mathbf{C}^b_n(\boldsymbol{\omega}^n_{ie} + \boldsymbol{\omega}^n_{en}). \tag{2}$$

C. IMU Noise Model

This paper considers eight different error sources for each sensor of an IMU, consisting of three accelerometers and three gyroscopes. The error sources include stochastic components of white noise, bias instability, and random walk; deterministic components of scale factor inconsistency, misalignment, and turn-on bias; and sensor limitations of FSR and bandwidth. These error sources are added to the noise-free accelerometers and gyroscopes readings described in (1) and (2).

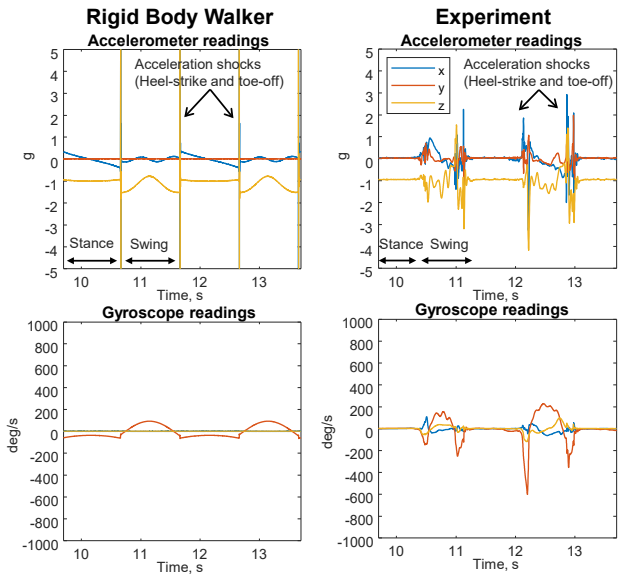

Fig. 2. Example profiles of simulated and measured IMU readings in two steps, in the case of walking along a straight line. The left column represents modeled sensors' readings, and the right column represents experimental sensors' readings.

1) Stochastic Noise Model: Simulated accelerometer readings corrupted with the stochastic components, denoted as $\hat{\mathbf{u}}_a$, are expressed as

$$\hat{\mathbf{u}}_a = \mathbf{u}_a + \hat{\mathbf{n}}_N + \hat{\mathbf{n}}_B + \hat{\mathbf{n}}_K, \tag{3}$$

where $\hat{\mathbf{n}}_N$, $\hat{\mathbf{n}}_B$, and $\hat{\mathbf{n}}_K$ denote the white noise, bias instability, and random walk components, respectively. This paper modeled these three noise components with approaches presented in [14], having the following formulations:

$$\hat{\mathbf{n}}_N = \boldsymbol{\omega}_N, \dot{\hat{\mathbf{n}}}_B = -\mu_B \hat{\mathbf{n}}_B + \boldsymbol{\omega}_B, \dot{\hat{\mathbf{n}}}_K = \boldsymbol{\omega}_K,$$

where $\boldsymbol{\omega}_N$, $\boldsymbol{\omega}_N$, and $\boldsymbol{\omega}_K$ are zero-mean Gaussian noise with variances of σ_N^2, σ_B^2, and σ_K^2, respectively. The values of the variances are to be determined via an optimization process that fits the noise models to the Allan Variance plot of a real IMU. μ_B is the correlation time associated with bias instability, and the value of μ_B was set to 10 [s] in this paper.

2) Deterministic Noise Model: Simulated accelerometer readings corrupted with both the stochastic and deterministic components, denoted as $\tilde{\mathbf{u}}_a$, are expressed as

$$\tilde{\mathbf{u}}_a = \mathbf{M}(\hat{\mathbf{u}}_a + \mathbf{b}_0), \tag{4}$$

where $\mathbf{M}$ is a misalignment matrix with diagonal entries being scale factor errors along the three axes and off-diagonal entries being cross-axis sensitivity, and $\mathbf{b}_0$ is the turn-on bias. In this paper, values of $\mathbf{b}_0$ were determined from a zero-mean Gaussian distribution with a variance of $\sigma_{\mathbf{b}_0}^2$ at the beginning of each simulation.

TABLE I
PARAMETER SETTINGS FOR DIFFERENT NOISE MODELS.

Parameter	Accel Value	Gyro Value
White noise σ_N	0.0015 [m/s$^{3/2}$]	1.74e−4 [rad/s$^{1/2}$]
Bias instability σ_B	3.92e−4 [m/s^2]	4.84e−5 [rad/s]
Random walk σ_K	1.01e−4 [m/s$^{5/2}$]	1.41e−4 [rad/s$^{3/2}$]
Scale factor error	0.05%	0.05%
Cross axis sensitivity	0.02°	0.02°
Turn-on bias $\sigma_{\mathbf{b}_0}$	0.01 [g]	0.3 [deg/s]
Full-scale range α_{FSR}	16 [g]	2000 [deg/s]
Bandwidth f_{cutoff}	260 [Hz]	256 [Hz]

3) Sensor Measurement Limitation: This paper applies a 6th-order Butterworth low-pass filter on $\tilde{\mathbf{u}}_a$ with a cut-off frequency, denoted as f_{cutoff}, to simulate the limited bandwidth of an IMU. To simulate sensor with limited FSR, α_{FSR}, we require that $|\tilde{\mathbf{u}}_a| < \alpha_{\text{FSR}}$. Simulated IMU readings that include the stochastic and deterministic noise components and measurement limitation, denoted as $\bar{\mathbf{u}}_a$, is expressed as

$$\bar{\mathbf{u}}_a = \begin{cases} \alpha_{\text{FSR}} & \text{if lowpass}(\tilde{\mathbf{u}}_a, f_{\text{cutoff}}) > \alpha_{\text{FSR}} \\ -\alpha_{\text{FSR}} & \text{if lowpass}(\tilde{\mathbf{u}}_a, f_{\text{cutoff}}) < -\alpha_{\text{FSR}} \\ \text{lowpass}(\tilde{\mathbf{u}}_a, f_{\text{cutoff}}) & \text{otherwise} \end{cases} \tag{5}$$

The processes described in (3)-(5) with different noise parameter settings are used to obtain simulated gyroscope readings corrupted with the error sources, denoted as $\bar{\mathbf{u}}_g$. In this paper, IMU readings were simulated based on noise characteristics of a VectorNav IMU VN-200. The parameters of stochastic noise components were determined experimentally with the Allan Variance test, and the deterministic component and sensor measurement limitation parameters were set nominally according to the sensor datasheet. Values of the parameters used in our proposed approach are summarized in TABLE I. The sampling rate of the simulated IMU was set to 800 [Hz].

Fig. 2 shows profiles of IMU readings in two steps generated with the proposed simulation and collected with a VN-200 IMU. In Fig. 2, acceleration shocks could be observed during the heel-strike and toe-off phases, in both the simulated and experimented IMU readings. The acceleration shocks in the simulation were generated because the rigid body walker model discussed in Section II-A considers events of the foot colliding with the ground, which causes a discontinuity in velocity measurements. The maximum acceleration shock generated in our model was around 200 [g].

III. EXPERIMENTAL VALIDATION

This paper compares the navigation accuracy of the ZUPT-aided INS using a series of 20 simulations and 20 experiments. In each run of the simulations, we used the model discussed in Section II-A with 28 steps, resulting in a straight-line trajectory of 42.86 [m]. In the experiments, an IMU VN-200 was mounted on the toe-side of a subject's boot, and the sampling rate of the sensor was set to 800 [Hz]. The subject walked a straight-line trajectory of 42.3 [m] with each step length of approximately 0.75 [m] and a pace of around 60 steps per minute. The ZUPT-aided INS was implemented in an Extended Kalman Filter (EKF) with the Acceleration-Moving Variance (AMV) detector [15]. The initial yaw angle of each navigation solution was assumed to be aligned with the North.

Fig. 3 shows the navigation results of the simulations (left column) and experiments (right column). 3D Root-Mean-Square-Error (RMSE), horizontal Circular Error Probable

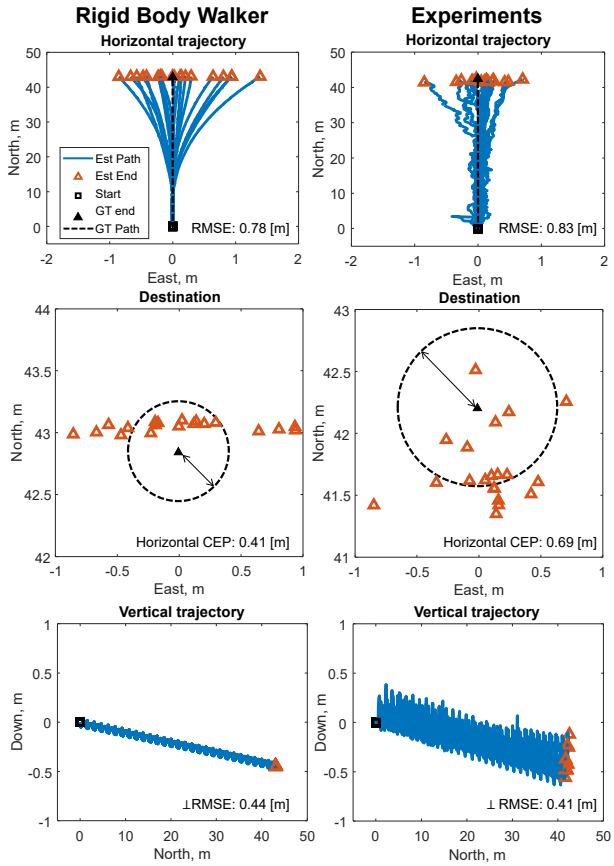

Fig. 3. Comparison of navigation accuracy of the ZUPT-aided INS in the cases of rigid body walker simulation and experiments with VN-200 IMU. The left column represents modeling, and the right column represents experiments.

(CEP), and vertical ($\perp$) RMSE between the simulated and experimental results had a difference of 6%, 40%, and 7%, respectively. The vertical positions in the simulations and experiments drifted in the same direction. To the best of our knowledge, this is the first pedestrian navigation simulation model that captures with sufficient accuracy the vertical positioning drifts. It could be shown with our model that insufficient sensor FSR and bandwidth are the dominating sources of the drifts. This observation supports the hypothesis on the causes leading to the vertical positioning drifts in the foot-mounted INS that were discussed in previous research [9].

Two lessons could be learned by observing the results presented in Fig. 3. First, the $\perp$ RMSE of the simulation results was larger than the experiments. This was due to the fact that the simulated accelerometer readings, as shown in Fig. 2, even though capturing the trend, had significantly larger shocks along the z-axis than the experimental accelerometer readings. When limiting in the simulated IMU readings the accelerometer FSR to 16 [g], large accelerometer biases were introduced, resulting in a larger vertical positioning error. Second, the estimated trajectory length in the experiments had larger deviations than in the simulation. We believe the reason is that the simulated IMU signals had identical patterns in each step, while, in the experiments, the signals had slightly different patterns of the human subject's walking style. Thus, a fixed threshold in the stance phase detection could be optimal in the simulation but not in the experiments. These observations suggest that, in order to improve the accuracy of navigation uncertainty prediction, future research should augment the model with more sophisticated foot motions. One potential research direction is to combine the analytical rigid body walker with traditional approaches of generating foot motion using motion cameras or IMUs.

IV. Conclusion

This paper proposed a simple, yet practical, model that is sufficient to predict with high accuracy the navigation uncertainty of a ZUPT-aided INS using a foot-mounted IMU. The experimental results showed that the proposed simulation model had a 6% discrepancy in position RMSEs, as compared to experiments, but captured all main features of motion. Our model also accurately predicted the drift in the vertical direction, matching well the reported experiments.

References

[1] D. Titterton, J. L. Weston, and J. Weston, *Strapdown inertial navigation technology*. IET, 2004, vol. 17.

[2] E. Foxlin, "Pedestrian tracking with shoe-mounted inertial sensors," *IEEE Computer Graphics and Applications*, vol. 25, no. 6, pp. 38–46, 2005.

[3] C.-S. Jao, A. A. Abdallah, C. Chen, M.-W. Seo, S. S. Kia, Z. M. Kassas, and A. M. Shkel, "PINDOC: Pedestrian indoor navigation system integrating deterministic, opportunistic, and cooperative functionalities," *IEEE Sensors Journal*, vol. 22, no. 14, pp. 14 424–14 435, 2022.

[4] T. T. Pham and Y. S. Suh, "Spline function simulation data generation for walking motion using foot-mounted inertial sensors," *Electronics*, vol. 8, no. 1, p. 18, 2018.

[5] A. D. Young, M. J. Ling, and D. K. Arvind, "IMUSim: A simulation environment for inertial sensing algorithm design and evaluation," in *ACM/IEEE International Conference on Information Processing in Sensor Networks*, Chicago, IL, USA, Apr. 12-14, 2011.

[6] Y. Wang, A. Chernyshoff, and A. M. Shkel, "Error analysis of ZUPT-aided pedestrian inertial navigation," in *International Conference on Indoor Positioning and Indoor Navigation*, Nantes, France, Sep. 24-27, 2018.

[7] F. J. Zampella, A. R. Jiménez, F. Seco, J. C. Prieto, and J. I. Guevara, "Simulation of foot-mounted IMU signals for the evaluation of PDR algorithms," in *International Conference on Indoor Positioning and Indoor Navigation*, Guimarães, Portugal, Sep. 21-23, 2011.

[8] C.-S. Jao and A. M. Shkel, "A reconstruction filter for saturated accelerometer signals due to insufficient FSR in foot-mounted inertial navigation system," *IEEE Sensors Journal*, vol. 22, no. 1, pp. 695–706, 2021.

[9] J. Wahlström and I. Skog, "Fifteen years of progress at zero velocity: A review," *IEEE Sensors Journal*, vol. 21, no. 2, pp. 1139–1151, 2020.

[10] M. Garcia, A. Chatterjee, A. Ruina, and M. Coleman, "The simplest walking model: stability, complexity, and scaling," *ASME Journal Biomechanical Engineering*, vol. 120, no. 2, pp. 281–288, 1998.

[11] A. D. Kuo, "A simple model of bipedal walking predicts the preferred speed–step length relationship," *ASME Journal Biomechanical Engineering*, vol. 123, no. 3, pp. 264–269, 2001.

[12] R. M. Alexander, "Simple Models of Human Movement," *Applied Mechanics Reviews*, vol. 48, no. 8, pp. 461–470, 08 1995. [Online]. Available: https://doi.org/10.1115/1.3005107

[13] A. Kuo, "Energetics of actively powered locomotion using the simplest walking model," *ASME Journal Biomechanical Engineering*, vol. 124, p. 113, 2002.

[14] J. A. Farrell, F. O. Silva, F. Rahman, and J. Wendel, "IMU Error Modeling for State Estimation and Sensor Calibration:A Tutorial," *IEEE Control Systems Magazine*, vol. 42, no. 6, pp. 40–66, 2021.

[15] I. Skog, P. Handel, J.-O. Nilsson, and J. Rantakokko, "Zero-velocity detection—an algorithm evaluation," *IEEE Transactions on Biomedical Engineering*, vol. 57, no. 11, pp. 2657–2666, 2010.